ISSN 0036-0244, Russian Journal of Physical Chemistry A, 2024, Vol. 98, No. 10, pp. 2186–2194. © Pleiades Publishing, Ltd., 2024.

CHEMICAL THERMODYNAMICS AND THERMOCHEMISTRY

Statistical Thermodynamic Analysis of the Effect of Chemical Composition on Changes in the Melting Temperatures of Alkali Metal Halides

A. G. Davydov[a,*]

[a] *Institute of High Temperature Electrochemistry, Ural Branch, Russian Academy of Sciences, Yekaterinburg, 620990 Russia*
**e-mail: A.Davydov@ihte.ru*

Received December 1, 2023; revised February 16, 2024; accepted February 19, 2024

Abstract—An interpretation is proposed for the dependence of the melting temperatures of an entire subclass of alkali metal halides on the chemical composition, based on an analysis of changes in different contributions to the internal energy of salts in the molten and crystalline phases with variation in the sum of the radii of their cations and anions. The expression for calculating the energy of liquid salt melts includes the contribution from charge–dipole interactions between ions, which is considered in a work based on thermodynamic perturbation theory with a basis in the form of a model of charged hard spheres. The Born–Mayer formula is used for the energy of the crystalline phase in the electrostatic part, while Debye's formula is employed to consider the contribution from vibrations. An explanation is given for the lower values of the reduced melting temperatures of lithium and sodium halides, relative to other salts. It is shown that deviations of the reduced melting temperatures of lithium and sodium halides depending on the sum of ionic radii can be explained by Coulomb and translational contributions to the energy in the molten state, along with Madelung and Born contributions in the crystalline phase.

Keywords: alkali metal halides, melting points, internal energy, thermodynamic perturbation theory, charged hard spheres, polarizability

DOI: 10.1134/S0036024424701322

INTRODUCTION

One of the most important tasks in the theory of molten salts from the viewpoint of practical application is predicting the conditions and boundaries of the stable existence of phases [1]. Theoretical approaches to describing the thermodynamic characteristics and phase equilibria in salt systems on basis of semiempirical modeling [2–7] and variations of quantum and molecular dynamics [8–12] are now being developed.

Despite the successes of computer modeling, means based on modern concepts of statistical thermodynamics have yet to be successfully applied to problems of describing thermodynamic properties and phase equilibria in salt melts. The classical statistical–thermodynamic approach would contribute to both a simpler calculation procedure and an understanding of patterns when, e.g., analyzing changes in melting points and other properties of salts with variations in composition, along with the reasons for the observed trends. Identifying such patterns is an important line in the field of physical chemistry. However, a comprehensive analysis of the dependence of melting temperatures on different contributions to the interionic interaction of melts and crystals upon changes in chemical composition has yet to be done even for the simplest subclass of alkali metal halides (AMH).

Since the main contribution to the interionic interaction of alkali metal halides is made by its Coulomb part [13], the value of which is determined by the differences in ionic radii between members of this family, it is logical to analyze the dependence of melting temperatures on the chemical composition of a material using simple values of the sum of and difference between the radii of the cation and anion salts In [14], we proposed a model that allowed us to calculate the melting temperatures of the entire AMH subclass by considering charge–dipole interactions in melts, using thermodynamic perturbation theory based on a charged hard sphere comparison system. We also showed that the melting temperatures of alkali metal halides have some common characteristic dependences on the sum of and difference between the radii of the cations and anions of the salts. However, a number of salts stood out sharply from the dependences noted in the work.

For a more accurate analysis of the dependence of melting temperatures on the cation–anion composition, it is advisable to consider not the entire AMH subclass, but its individual subgroups. It is then most

logical to analyze such dependences based mainly on the sum of the radii of cations and anions. Emphasis in this work will therefore be placed on analyzing and explaining trends of changes in the melting temperatures of individual AMH subgroups with common cations, depending on the sum of the ionic radii of the salts. However, it is worth noting that an interesting task for further consideration beyond the scope of this work would be analyzing the melting temperatures of a given subclass of salts depending on, e.g., the difference between or ratio of the radii of the AMH ions.

THEORETICAL

It is well known that the melting point of any system can be represented as the ratio of the change in enthalpy to the change in entropy during a phase transition:

$$T_m = \frac{\Delta H_m}{\Delta S_m} \text{ [15].}$$

At pressures of the order of 1 atm, the change in the enthalpy of salts is almost equal to the change in their internal energy:

$$T_m = \frac{\Delta H_m}{\Delta S_m} \cong \frac{\Delta E_m}{\Delta S_m}.$$

At the same time, the change in entropy during melting of an AMH crystal can be considered approximately constant:

$$\Delta S_m \approx 3Nk_B \text{ [16],}$$

where N is the number of particles in the mixture and k_B is the Boltzmann constant. The melting temperature of the alkali halide salt should then be determined mainly by the energy difference between the melt and the crystal:

$$T_m = \frac{\Delta E_m}{\text{const}} = \frac{E_{liq} - E_{sol}}{\text{const}}.$$

For a theoretical analysis of the dependence of melting temperatures on the cation–anion composition of AMH, it is therefore interesting to consider their relationship with different contributions to the internal energy of the corresponding melts and crystals.

Let us now turn to describing the model for calculating different contributions to the internal energy of AMH melts and crystals. We shall consider an alkali-halide melt as an ionic mixture consisting of an equal number ($N_1 = N_2 = 1/2N$) of cations Me^+ with charge $+1e$ and anions X^- with charge $-1e$ (where $Me^+ = Li^+$, Na^+, K^+, Rb^+, Cs^+, and $X^- = F^-$, Cl^-, Br^-, I^-). We determine the fraction of ith grade ions in a mixture as $x_i = N_i/N = 1/2$; cation and anion diameters as d_1 and d_2, respectively; and the sum of their radii as $d = 1/2(d_1 + d_2)$.

The internal energy of a liquid melt can be presented as the sum

$$E_{liq} = E_{tr} + E_q + E_{pol}, \quad (1)$$

where $E_{tr} = (3/2)Nk_BT$ is the contribution from translational degrees of freedom to the energy [17]; E_q is the Coulomb contribution; and E_{pol} is the charge–dipole correction to the energy of the reference system.

The Coulomb contribution to the internal energy was found in Blum's work within the mean-spherical approximation for a multisort mixture of charged hard spheres [18]. The expression for energy in this case has the form

$$E_q = -\frac{Ne^2}{\varepsilon}\left[\sum_i \frac{x_i Z_i^2 \Gamma}{1+\Gamma d_i} + \frac{\pi P_n^2}{2\Delta}\frac{\Omega}{\rho}\right]. \quad (2)$$

Here, e is the elementary charge; ε is the dielectric constant; Z_i is the formal charge of the ith ion; $\Delta = 1 - \eta$, where $\eta = \pi\rho_i d_i^3/6$ is the packing factor; $\rho_i = x_i\rho$ is the partial numerical density of the ith ion; $\rho = N/V$ is the numerical density; and V is the volume of the mixture. Parameter Γ included in expression (2) describes the decay decrement of charge density oscillations around the central ion:

$$\Gamma^2 = \frac{\pi e^2}{\varepsilon k_B T}\sum_i \rho_i X_i^2, \quad \text{where} \quad X_i = \frac{Z_i - \frac{\pi d_i^2}{2\Delta}P_n}{1+\Gamma d_i}. \quad (3)$$

The relations for auxiliary quantities introduced to solve the mean-spherical model have the form [19]

$$P_n = \frac{\rho}{\Omega}\sum_i \frac{x_i Z_i d_i}{1+\Gamma d_i}, \quad \Omega = 1 + \frac{\pi\rho}{2\Delta}\sum_i \frac{x_i d_i^3}{1+\Gamma d_i}. \quad (4)$$

Expressions (1)–(4) determine the energy of the comparison system of charged hard spheres at a given density and temperature. It is reasonable to redirect the problem of considering additional effects into energy to the thermodynamic perturbation theory [20], which allows us to consider the second-order charge–dipole correction to the interaction of ions according to quantum mechanical theory as a small perturbation in the potential energy of the comparison system of charged hard spheres, using its structural factors as a basis:

$$E_{pol} = \frac{N}{4\pi^2}\sum_{i,j}\sqrt{x_i x_j}\int_0^\infty \varphi_{ij}^{pol}(k)\left(S_{ij}^{chs}(k) - \delta_{ij}\right)k^2 dk + \frac{N\rho}{2}\sum_{i,j} x_i x_j \varphi_{ij}^{pol}(0), \quad (5)$$

where δ_{ij} is the Kronecker delta; k is the wave number; $\varphi_{ij}^{pol}(k)$ is the Fourier image of the disturbance; and

$S_{ij}^{\text{chs}}(k)$ represents partial structural factors for a two-grade mixture:

$$S_{ii}(k) = \frac{1-\rho_j\tilde{c}_{jj}(k)}{(1-\rho_i\tilde{c}_{ii}(k))(1-\rho_j\tilde{c}_{jj}(k))-(\rho_{ij}\tilde{c}_{ij}(k))^2};$$
$$S_{ij}(k) = \frac{\rho_{ij}\tilde{c}_{ij}(k)}{(1-\rho_i\tilde{c}_{ii}(k))(1-\rho_j\tilde{c}_{jj}(k))-(\rho_{ij}\tilde{c}_{ij}(k))^2}. \quad (6)$$

Here, $\rho_{ij} = \sqrt{\rho_i\rho_j}$, $\tilde{c}_{ij}(k)$ are direct correlation functions of the mean-spherical model in Fourier space [14].

The Fourier image of the perturbing charge–dipole part of the pair potential can be reduced to the form

$$\varphi_{ij}^{\text{pol}}(k) = \pi k E_{ij} \times\left[\frac{\sin(kd_{ij})}{k^2d_{ij}^2}+\frac{\cos(kd_{ij})}{kd_{ij}}+\text{Si}(kd_{ij})-\frac{\pi}{2}\right], \quad (7)$$

where $\text{Si}(kd_{ij})$ is an integral sine. E_{ij} describes the characteristic value of the charge–dipole interaction of a pair of ions and is determined by the expression [13]

$$E_{ij} = \frac{Z_i^2e^2b_j^3}{\varepsilon}\frac{(\varepsilon-1)b_j^3-(\varepsilon+2)\alpha_j}{(2\varepsilon+1)b_j^3-2(\varepsilon-1)\alpha_j} + \frac{Z_j^2e^2b_i^3}{\varepsilon}\frac{(\varepsilon-1)b_i^3-(\varepsilon+2)\alpha_i}{(2\varepsilon+1)b_i^3-2(\varepsilon-1)\alpha_i}. \quad (8)$$

Here, α_i is the polarizability of the ith ion; b_i is the radius of its Born cavity, which can naturally be equated to the ionic radius ($R_i = d_i/2$). To calculate the dielectric constant, we use the standard Clausius–Mossotti formula, which agrees well with data obtained from refractive indices, at least for melts of alkali metal halides [13]:

$$\varepsilon = \frac{3}{1-\frac{4\pi\rho}{3}\sum_i x_i\alpha_i}-2. \quad (9)$$

To calculate the energies of alkali halide crystals, we used the Born–Mayer formula [21], which includes the Madelung energy and the Born correction for the repulsion of electron shells. The additional vibrational contribution to the energy was considered using the Debye model [22]:

$$E_{\text{sol}} = -\frac{A_{\text{M}}Ne^2}{2R_0}\left(1-\frac{\rho_{\text{B}}}{R_0}\right) + \frac{9}{8}Nk_{\text{B}}T\left(\frac{8}{\theta_{\text{D}}^3}\int_0^{\theta_{\text{D}}}\frac{\theta_{\text{D}}^3d\theta_{\text{D}}}{\exp(\theta_{\text{D}})-1}+\theta_{\text{D}}\right). \quad (10)$$

Here, A_{M} is the Madelung constant; ρ_{B} is the Born repulsion parameter; R_0 is the equilibrium interionic distance in the crystal; $\theta_{\text{D}} = \Theta_{\text{D}}/T$ is the reduced Debye temperature; and Θ_{D} is the characteristic Debye temperature. When calculating the corresponding contributions to the crystal energy, we used literature data on characteristic Debye temperatures [23], Born repulsion parameters in AMH crystals [24], Fumi–Toshi ionic radii [25], and Madelung constants [26]. As the initial parameters describing the pairwise interaction of ions in a melt, we took the tabulated values of the Fumi–Toshi radii [25] along with reference data on the Pauling polarizabilities [27] for all ions except the fluoride anion. Its polarizability (1.56 Å^3) was refined in [28] and used in this work.

RESULTS AND DISCUSSION

Let us consider the melting temperature reduced to the characteristic Coulomb energy:

$$T_m^* = k_{\text{B}}T_m\varepsilon_0d/e^2,$$

where ε_0 is the dielectric constant in a vacuum. This quantity is dimensionless, and the technique is usually used in theoretical works on phase transitions [29]. Figure 1a presents experimental values of reduced melting temperatures for individual AMH subgroups with common cations, taken from [30]. We can see their dependences on the sum of ionic radii are virtually linear, but have different slopes upon moving from lithium halides to cesium salts. This does not allow us to describe the melting temperatures of the entire AMH subclass from a unified position. The change in the slope of the dependences can be presented more clearly if we bring them to a single scale, assigning the sums of ionic radii (along the abscissa axis) and melting temperatures (along the ordinate axis) of each subgroup of salts of lithium, sodium, potassium, rubidium, and cesium halides to the corresponding values for alkali metal fluorides, and taking them as reference points. Such dependences are presented in Fig. 1b. We can see that the slope of the dependences for lithium and sodium halides is negative, but becomes increasingly positive upon moving to cesium halides. To understand the reasons for this behavior of the melting temperatures of AMH, we must consider the dependences of different contributions to the internal energies of their melts and crystals. Such dependences are therefore considered below in a key similar to Fig. 1.

Figure 2a presents dependences Δ of the total reduced internal energy of molten alkali metal halides, calculated using the proposed approach: $\Delta E_{\text{liq}}^* = \Delta E_{\text{liq}}\varepsilon_0d/e^2$ on the sum of ion radii. As with the melting temperatures of salts, Fig. 2b shows the relative dependences of energy on size, already reduced to the values calculated for alkali metal fluorides.

We can see that the slopes of these dependences are quite close and do not allow us to judge the reasons for the noted behavior of the AMH melting temperatures. We must therefore consider similar dependences for individual contributions to the internal energy of all melts, starting with the main Coulomb contribution. However, it is worth noting that the dependences

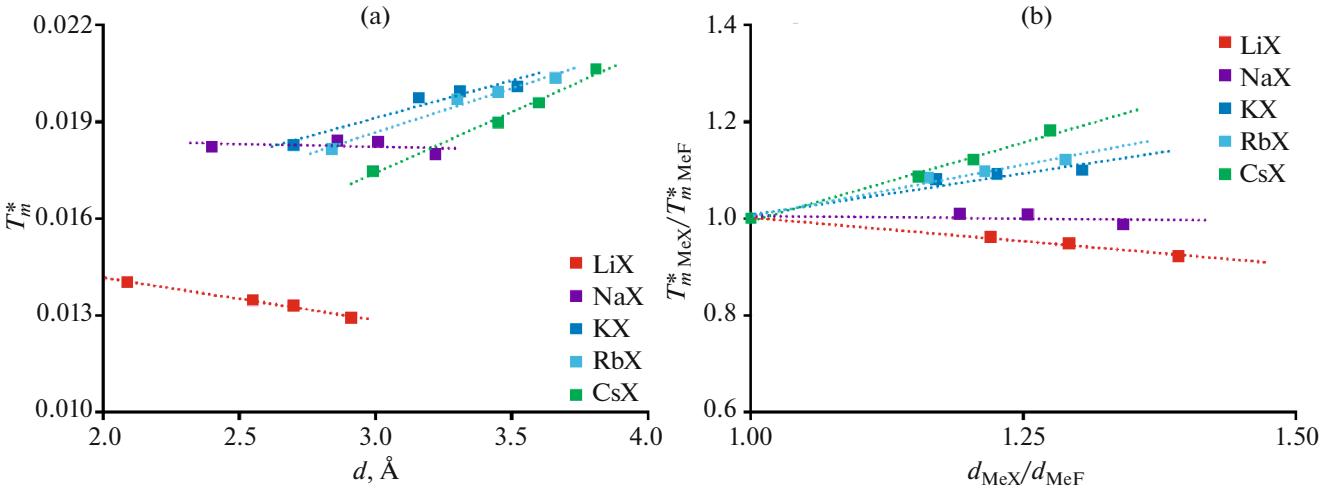

Fig. 1. (a) Experimental values of the reduced melting temperatures of alkali metal halides $T_m^* = k_B T_m \varepsilon_0 d/e^2$, depending on the sum of the radii of cations and anions of individual salts d and (b) the reduced melting temperatures of lithium, sodium, potassium, rubidium, and cesium halides, relative to the melting temperatures of the corresponding alkali metal fluorides, depending on the ratio of the sum of the radii of the ions of each salt to the sum of the radii of the ions of similar fluoride salts.

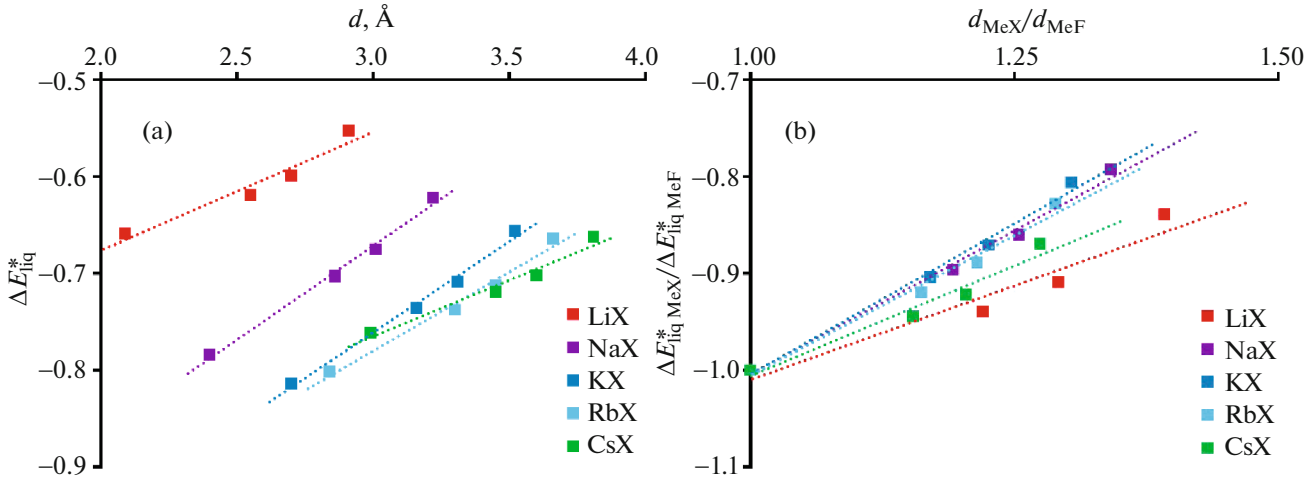

Fig. 2. (a) Results from calculating the reduced internal energies of molten alkali metal halides $\Delta E_{liq}^* = \Delta E_{liq} \varepsilon_0 d/e^2$, depending on the sum of the radii of cations and anions of individual salts d and (b) the values of the reduced internal energies of molten lithium, sodium, potassium, rubidium, and cesium halides, relative to the internal energies of the corresponding alkali metal fluorides, depending on the ratio of the sum of the radii of the ions of each salt to the sum of the radii of the ions of similar fluoride salts.

obtained for sodium, potassium, and rubidium halides virtually merge in the slope in Fig. 2b, while that of the dependences for cesium halides is even closer to liquid lithium halides.

Figure 3a presents results from calculating the Coulomb contribution to the reduced internal energy of individual subgroups of alkali metal halides, depending on the sum of ion radii. Figure 3b gives their relative values with respect to fluoride melts.

We can see it is the Coulomb contribution that sets the main trend in the dependence of the total internal energy of melts on composition. The slopes of the dependences are quite close for most subgroups, but that of lithium halides is the shallowest. To some extent, this contributes to the drop in the melting temperatures upon transitioning from lithium fluoride to iodide, due to the greater decline in the internal energy of melts with a large anion.

Let us also consider the translational contribution to the internal energy of AMH melts, results from calculating which are presented in Fig. 4.

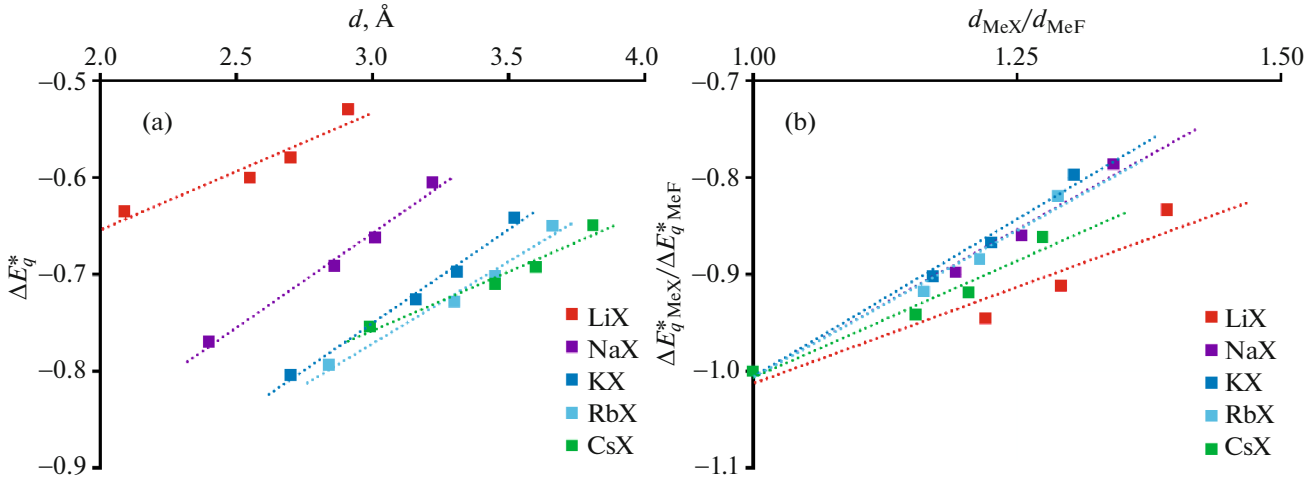

Fig. 3. (a) Results from calculating the Coulomb contribution to the reduced internal energy of molten alkali metal halides $\Delta E_q^* = \Delta E_q \varepsilon_0 d/e^2$, depending on the sum of the radii of cations and anions of individual salts d and (b) the values of this contribution to the reduced internal energy of molten lithium, sodium, potassium, rubidium, and cesium halides, relative to the Coulomb contribution to the internal energy of the corresponding alkali metal fluorides, depending on the ratio of the sum of the radii of the ions of each salt to the sum of the radii of the ions of similar fluoride salts.

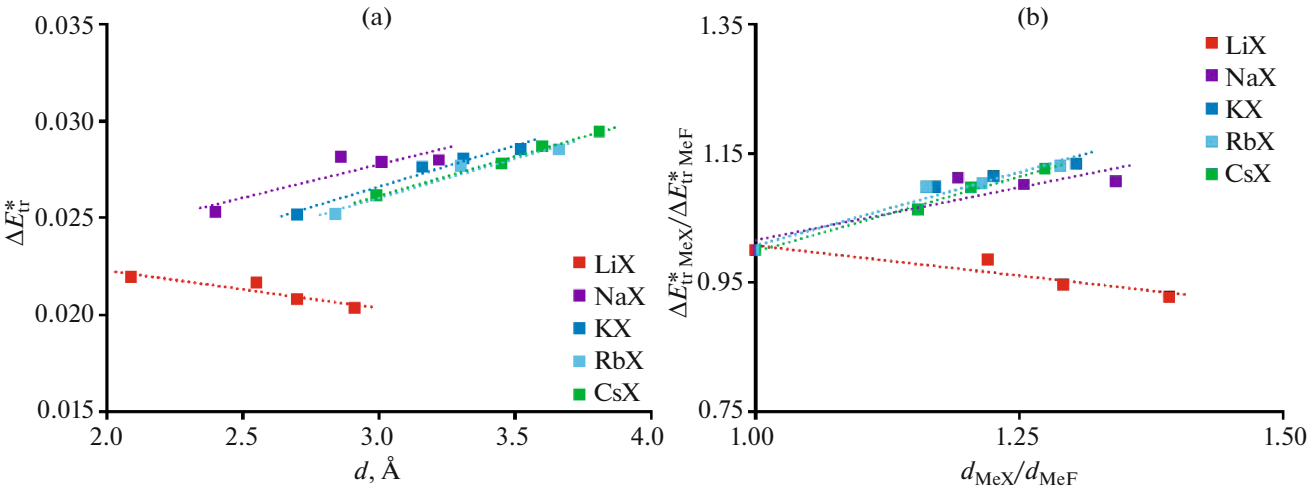

Fig. 4. (a) Results from calculating the translational contribution to the reduced internal energy of molten alkali metal halides $\Delta E_{tr}^* = \Delta E_{tr} \varepsilon_0 d/e^2$ depending on the sum of the radii of cations and anions of individual salts d and (b) the values of this contribution to the reduced internal energy of molten lithium, sodium, potassium, rubidium, and cesium halides, relative to the translational contribution to the internal energy of the corresponding alkali metal fluorides depending on the ratio of the sum of the radii of the ions of each salt to the sum of the radii of the ions of similar fluoride salts.

Figure 4 shows the dependences of the contribution from translational degrees of freedom for lithium and sodium halides have a shallower slope than those of other salts. The slope for lithium halides is even more negative, resulting in an additional drop in the internal energy of melts upon moving from fluorides to lithium iodides, which in turn contributes to the decline in their melting temperatures. However, the contribution from translational degrees of freedom to the melt energy is much smaller than that of Coulomb interaction, and therefore less dramatically affects the dependence of the AMH melting temperatures.

Finally, let us consider the charge–dipole contribution to the internal energy of AMH melts, the dependences of which are presented in Fig. 5. It is worth noting that only the charge–dipole contribution to the energy presents nonlinear dependences during the transition from fluorides to iodides of alkali metals. In the case of lithium salts, the energy of this inter-

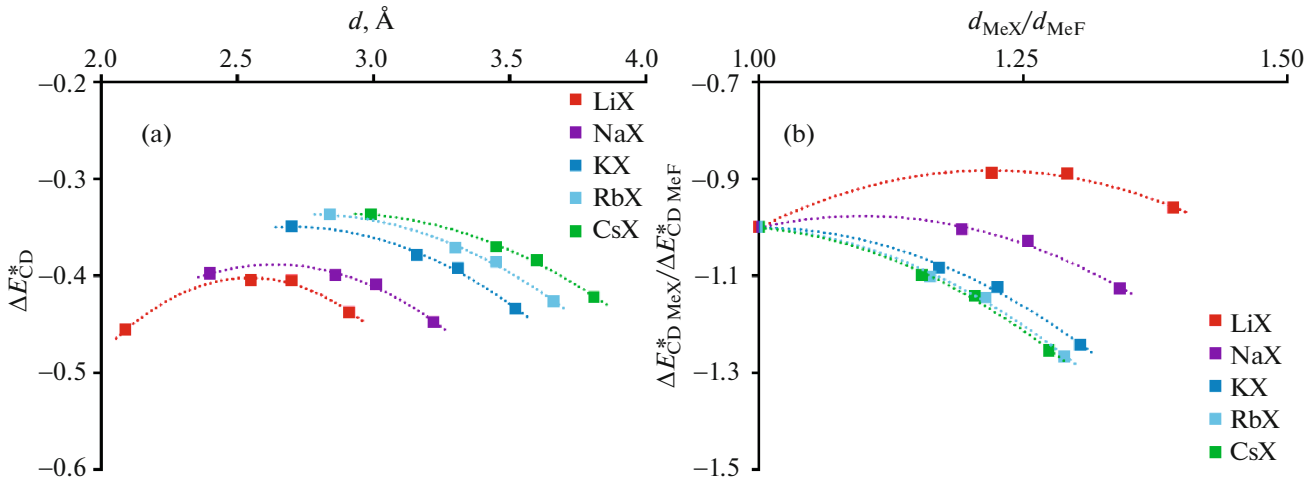

Fig. 5. (a) Results from calculating the charge–dipole contribution to the reduced internal energy of molten alkali metal halides $\Delta E^*_{CD} = \Delta E_{CD}\varepsilon_0 d/e^2$, depending on the sum of the radii of cations and anions of individual salts d and (b) the values of this contribution to the reduced internal energy of molten lithium, sodium, potassium, rubidium, and cesium halides, relative to the charge–dipole contribution to the internal energy of the corresponding alkali metal fluorides, depending on the ratio of the sum of the radii of the ions of each salt to the sum of the radii of the ions of similar fluoride salts.

action is maximal for its chlorides and bromides, relative to lithium fluoride and iodide.

It is generally seen that the calculated values of the charge–dipole contribution to the reduced internal energy for all AMH subgroups with common cations are quite close to one another and are an order of magnitude smaller than the Coulomb contribution to the energy of the melts (Fig. 5a). At the same time, the contribution from charge–dipole interactions somewhat violates the patterns noted for the two previous contributions, resulting in a greater increase in the internal energy in melts containing larger halide anions upon transitioning from cesium salts to cesium salts lithium (Fig. 5b). This contributes to a slight increase in the melting temperatures of lithium and sodium chlorides, bromides, and iodides, relative to other salts, or to partial compensation for the two contributions to the energy of melts discussed above.

Let us now analyze results from calculating the energy of AMH crystals. Figure 6 presents dependences similar to those in Fig. 2, but already describing the total reduced internal energy of individual subgroups of alkali halide crystals with the same cations.

It is clear that the magnitude and slope of the dependences for the calculated values of the internal energy of crystalline lithium halides differs significantly from other AMH crystals by being more positive and growing more sharply in the transition from fluorides to lithium iodides. A similar but less pronounced trend is observed for sodium halides, relative to the other considered crystals. The main reason for the slight drop in the reduced melting temperatures during the transition from fluorides to lithium and sodium iodides obviously lies in the energies of their crystalline phases, as will be shown when considering individual contributions.

Figure 7a presents results from calculating the Coulomb contribution to the reduced internal energy of AMH crystals, depending on the sum of ionic radii. Figure 7b gives their values, relative to the ones obtained for fluorides of each alkali metal.

We can see from Fig. 7 that the dependences of the reduced Madelung energy for all subgroups of crystals (except for lithium halides) are virtually identical in both their magnitude and their slope. Lithium halides, which have more positive energy values that grow considerably upon moving from fluorides to iodides, fall out of the general trend quite strongly. It is obviously this factor that is mainly responsible for the lower melting temperatures of lithium halides and their even greater drop as the size of the anion in the salt composition rises.

Figure 8 presents results from calculating the Born contribution from electron shell repulsion to the reduced energy of AMH crystals.

We can see that the values and the slope of the dependences in Fig. 8 for lithium, potassium, rubidium, and cesium halides are virtually identical, while sodium halides fall out of the general trend. The value of the Born contribution to the energy of these salts is more positive and falls less than that of the other melts during the transition from fluorides to iodides. This is apparently another key factor for the weaker increase in the reduced melting temperatures for sodium salts when considering systems with larger anions.

Finally, let us consider the last contribution to the energy of crystalline alkali metal halides. Figure 9 presents results from calculating the Debye vibrational

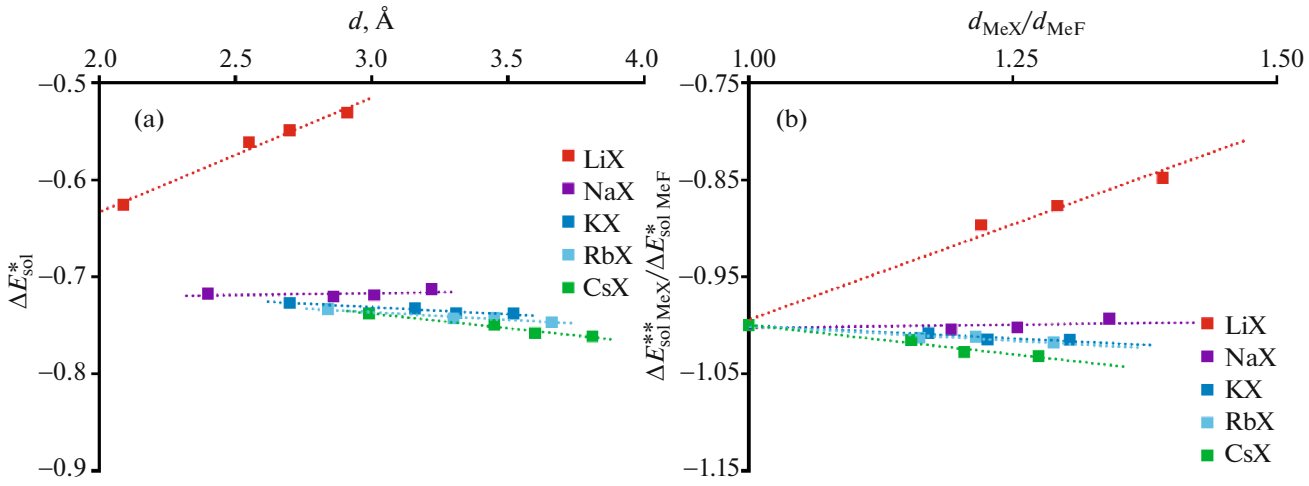

Fig. 6. (a) Results from calculating the reduced internal energies of crystals of alkali metal halides $\Delta E^*_{sol} = \Delta E_{sol}\varepsilon_0 d/e^2$, depending on the sum of the radii of cations and anions of individual salts d and (b) the values of the reduced internal energies of crystals of lithium, sodium, potassium, rubidium, and cesium halides, relative to the internal energies of the corresponding alkali metal fluorides, depending on the ratio of the sum of the radii of the ions of each salt to the sum of the radii of the ions of similar fluoride salts.

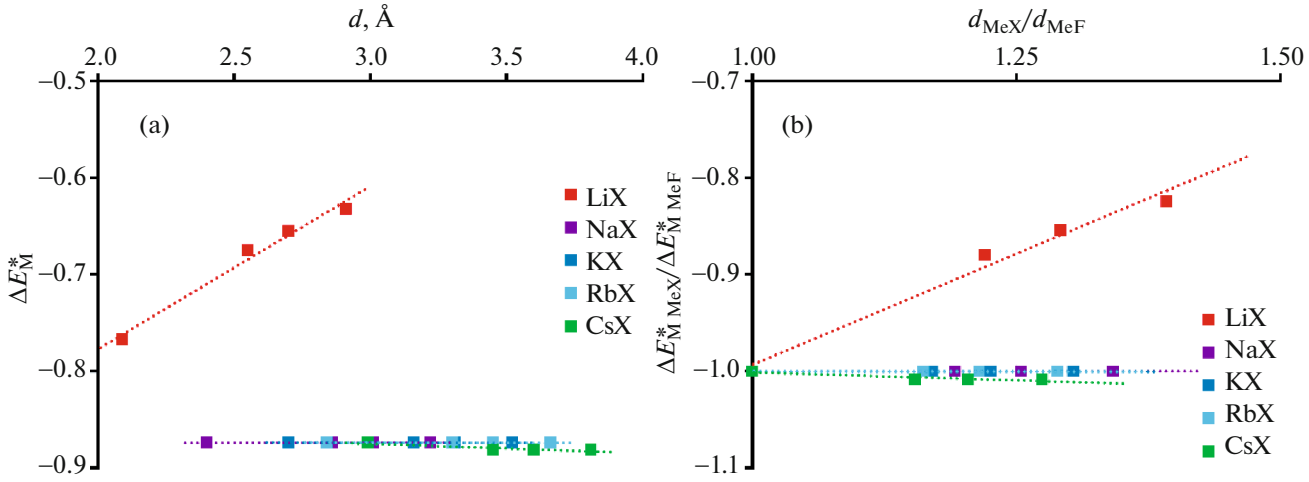

Fig. 7. (a) Results from calculating the Coulomb contribution (Madelung) to the reduced internal energy of crystals of alkali metal halides $\Delta E^*_M = \Delta E_M\varepsilon_0 d/e^2$, depending on the sum of the radii of cations and anions of individual salts d and (b) the values of this contribution to the reduced internal energy of crystals of lithium, sodium, potassium, rubidium, and cesium halides, relative to the Coulomb contribution to the internal energy of the corresponding alkali metal fluorides, depending on the ratio of the sum of the radii of the ions of each salt to the sum of the radii of the ions of similar fluoride salts.

contribution to the reduced internal energy of AMH crystals, depending on the sum of the radii of the cation and anion (Fig. 9a), and their values relative to those of alkali metal fluorides (Fig. 9b).

We can see the vibrational contribution tends to partially compensate for the Coulomb and Born interactions by reducing the vibrational energy during the transition from fluorides to iodides for lithium and sodium halides, relative to other crystals. However, this contribution is the one lowest in magnitude and therefore can have no appreciable effect on the dependences of the reduced melting temperatures of these salts.

CONCLUSIONS

The combination of contributions of different magnitudes and signs to the internal energy of AMH melts and crystals produces complex but analyzable results. Considering individual contributions to energy for

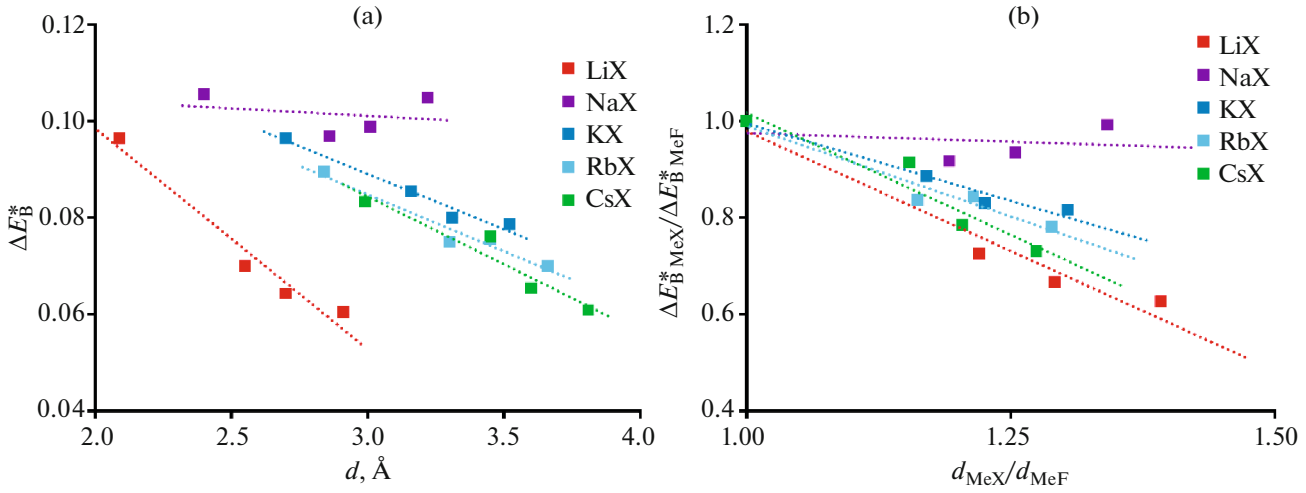

Fig. 8. (a) Results from calculating the repulsive contribution (Born) to the reduced internal energy of crystals of alkali metal halides $\Delta E^*_B = \Delta E_B \varepsilon_0 d/e^2$, depending on the sum of the radii of cations and anions of individual salts d and (b) the values of this contribution to the reduced internal energy of crystals of lithium, sodium, potassium, rubidium, and cesium halides, relative to the Born contribution to the internal energy of the corresponding alkali metal fluorides, depending on the ratio of the sum of the radii of the ions of each salt to the sum of the radii of the ions of similar fluoride salts.

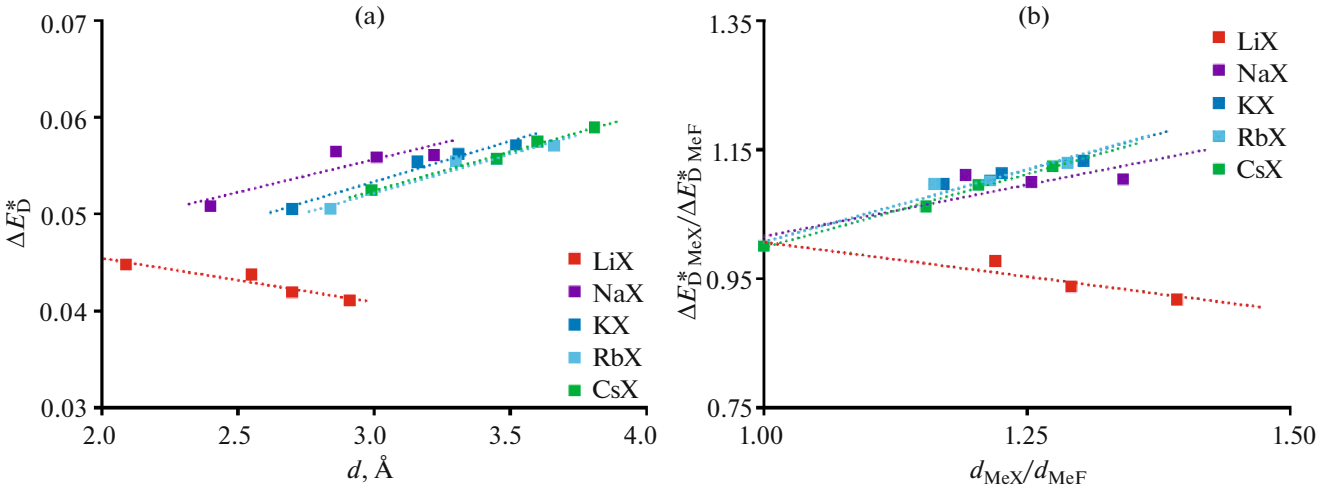

Fig. 9. (a) Results from calculating the vibrational contribution (Debye) to the reduced internal energy of crystals of alkali metal halides $\Delta E^*_D = \Delta E_D \varepsilon_0 d/e^2$, depending on the sum of the radii of cations and anions of individual salts d and (b) the values of this contribution to the reduced internal energy of crystals of lithium, sodium, potassium, rubidium, and cesium halides, relative to the Debye contribution to the internal energy of the corresponding alkali metal fluorides, depending on the ratio of the sum of the radii of the ions of each salt to the sum of the radii of the ions of similar fluoride salts.

individual subgroups of melts allows us to identify their relationship upon changes in the melting temperatures of alkali metal halides.

It was shown for potassium, rubidium, and cesium halides that the dependences of both the reduced melting temperatures and the main contributions to the internal energy of the phases were quite close in trend. At the same time, deviations of similar melting temperature dependences for lithium and sodium halides can easily be explained by Coulomb and translational contributions to the energy in the molten state, in addition to Madelung and Born contributions in the crystal phase. Depending on the hierarchy of these contributions to the internal energy, this interpretation produces a completely understandable and consistent explanation of the change in the melting temperatures of alkali metal halides.

ACKNOWLEDGMENTS

The author is grateful to Dr. Nikolai Konstantinovich Tkachev, Chief Researcher at the Smirnov Molten Salts Laboratory of the Institute of High-Temperature Electrochemistry, for his contribution to developing the concept of this work.

FUNDING

This work was supported by ongoing institutional funding. No additional grants to carry out or direct this particular research were obtained.

CONFLICT OF INTEREST

The author of this work declares that he has no conflicts of interest.

REFERENCES

1. F. Lantelme and H. Groult, *Molten Salts Chemistry: From Lab to Applications* (Elsevier, Amsterdam, 2013).
2. Y. A. Chang, S. Chen, F. Zhang, et al., Prog. Mater. Sci. **49**, 313 (2004). https://doi.org/10.1016/s0079-6425(03)00025-2
3. P. Chartrand and A. D. Pelton, Metall. Mater. Trans. A **32**, 1397 (2001). https://doi.org/10.1007/s11661-001-0229-0
4. X. Xing, Z. Zhu, S. Dai, and T. Tanaka, Thermochim. Acta **372**, 109 (2001). https://doi.org/10.1016/s0040-6031(01)00441-5
5. J. Kapała, M. Bochyńska, K. Broczkowska, and I. Rutkowska, J. Alloys Compd. **451**, 679 (2008). https://doi.org/10.1016/j.jallcom.2007.04.085
6. W. Gong, Y. Wu, R. Zhang, and M. Gaune-Escard, Calphad **36**, 44 (2012). https://doi.org/10.1016/j.calphad.2011.11.001
7. B. Kubíková, J. Mlynáriková, O. Beneš, et al., J. Mol. Liq. **268**, 754 (2018). https://doi.org/10.1016/j.molliq.2018.07.114
8. O. Beneš, Ph. Zeller, M. Salanne, and R. J. M. Konings, J. Chem. Phys. **130**, 134716 (2009). https://doi.org/10.1063/1.3097550
9. J. L. Aragones, E. Sanz, C. Valeriani, and C. Vega, J. Chem. Phys. **137**, 104507 (2012). https://doi.org/10.1063/1.4745205
10. L. C. Dewan, C. Simon, P. A. Madden, et al., J. Nucl. Mater. **434**, 322 (2013). https://doi.org/10.1016/j.jnucmat.2012.12.006
11. R. S. DeFever, H. Wang, Y. Zhang, and E. J. Maginn, J. Chem. Phys. **153**, 011101 (2020). https://doi.org/10.1063/5.0012253
12. H. Wang, R. S. DeFever, Y. Zhang, et al., J. Chem. Phys. **153**, 214502 (2020). https://doi.org/10.1063/5.0023225
13. F. H. Stillinger, *Equilibrium Theory of Pure Fused Salts* (Wiley, New York, 1964).
14. A. G. Davydov and N. K. Tkachev, Rasplavy, No. 2, 167 (2023). https://doi.org/10.31857/S0235010623020032
15. I. Prigogine and R. Defay, *Chemical Thermodynamics* (Longmans, London, 1954).
16. *Molten Salt Chemistry,* Ed. by M. Blander (Interscience, New York, 1964).
17. L. D. Landau and E. M. Lifshitz, *Course of Theoretical Physics,* Vol. 5: *Statistical Physics* (Pergamon, Oxford, 1980).
18. L. Blum, *Primitive Electrolytes in the Mean Spherical Approximation* (Academic, New York, 1980).
19. K. Hiroike, Mol. Phys. **33**, 1195 (1977). https://doi.org/10.1080/00268977700101011
20. J. R. Solana, *Perturbation Theories for the Thermodynamic Properties of Fluids and Solids* (CRC, Taylor Francis Group, Boca Raton, 2013).
21. M. Born and J. E. Mayer, Z. Phys. **75**, 1 (1932).
22. J. E. Mayer and M. G. Mayer, *Statistical Mechanics* (Wiley, Chichester, 1940).
23. M. N. Magomedov, Teplofiz. Vys. Temp. **30**, 1110 (1992).
24. D. B. Sirdeshmukh, L. Sirdeshmukh, and K. G. Subhadra, *Alkali Halides: A Handbook of Physical Properties* (Springer, Berlin, 2001).
25. M. P. Tosi and F. G. Fumi, J. Phys. Chem. Solids **25**, 45 (1964). https://doi.org/10.1016/0022-3697(64)90160-x
26. N. W. Ashcroft and N. D. Mermin, *Solid State Physics* (Harcourt College Publ., Philadelphia, 1976).
27. S. S. Batsanov and A. S. Batsanov, *Introduction to Structural Chemistry* (Springer Science, New York, 2012).
28. J. N. Wilson and R. M. Curtis, J. Phys. Chem. **74**, 187 (1970). https://doi.org/10.1021/j100696a034
29. M. E. Fisher, J. Stat. Phys. **75**, 1 (1994). https://doi.org/10.1007/BF02186278
30. W. M. Haynes, *CRC Handbook of Chemistry and Physics,* 97th ed. (CRC, Taylor Francis Group, Boca Raton, 2017).